

# Deciphering the role of accessory proteins in *Arabidopsis* chloroplast editosomes via interaction with a synthetic PPR-PLS factor in *E. coli*

Jose M. Lombana , Maureen R. Hanson , Stéphane Bentolila \*

Department of Molecular Biology and Genetics, Cornell University, Ithaca, NY 14853, United States

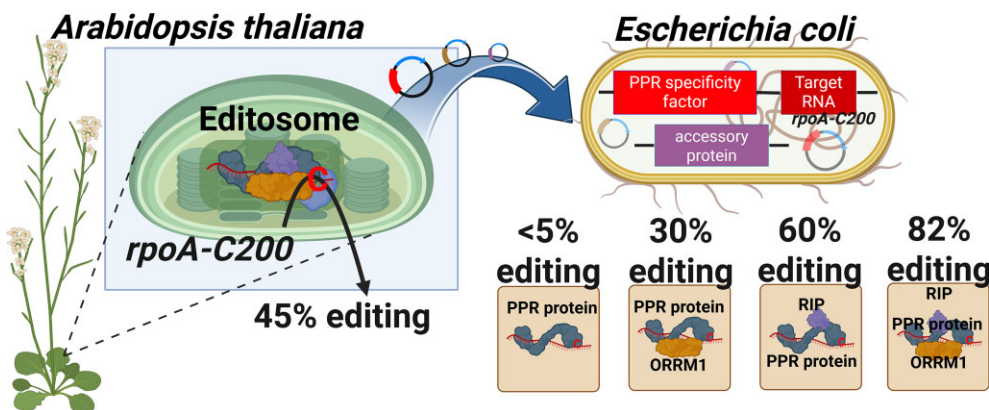
\*To whom correspondence should be addressed. Email: sb46@cornell.edu

Downloaded from https://academic.oup.com/nar/article/53/1/gkaf483/8160309 by Cornell University user on 04 September 2025

## Abstract

RNA editing modifies cytidines to uridines in plant organelle transcripts so that their sequences differ from the ones predicted from the genomic DNA. This process involves a family of RNA-binding proteins that has significantly expanded, the pentatricopeptide repeat (PPR)-containing proteins. In angiosperms, PPR proteins are found in editosomes associated with accessory proteins. The exact function of these accessory proteins has been unclear. Bacterial co-expression of an angiosperm synthetic factor and different accessory proteins, RIP2, RIP9, and ORRM1, demonstrates their essential role in editing of an RNA target. The presence of ORRM1 and RIP2 or ORRM1 and RIP9 in bacteria with the PPR factor results in a target editing extent of 80%, which is similar to what is observed *in planta*. Accessory proteins increase the affinity of the PPR factor for the target RNA, likely the explanation of their role in improving editing efficiency. RNA-seq analysis of bacterial transcriptome in samples expressing various combinations of accessory proteins along with the synthetic factor identified a total of 34 off-target editing events. Investigation of their upstream sequences that are recognized and bound by the synthetic factor will facilitate the optimization of future designs to improve the specificity of this programmable RNA-editing factor.

## Graphical abstract



## Introduction

Among the post-transcriptional processes that influence gene expression, C-to-U RNA editing in plants exhibits several unique features. Editing in plants is restricted to genome-containing organelles—chloroplasts and mitochondria. Unlike other types of RNA editing, the purpose of plant RNA editing is not to generate multiple proteins from the same transcript; instead, its role is to rectify T-to-C mutations in critical locations of transcripts, ensuring the production of functional proteins [1]. A typical vascular plant requires over 600 RNA editing-mediated corrections in its organelle transcripts [2]. While previous research has shed some light on the editing mechanism, there is still much to be discovered—information

that may eventually enable the biotechnological exploitation of this phenomenon.

How do plants achieve so many specific changes from Cs to Us? Through evolution, a modular family of RNA-binding proteins has significantly expanded, often comprising over 400 members in a single plant species [3]. Pentatricopeptide repeats (PPR), 35 amino-acid repeats present in tandem, can bind RNA in a sequence-specific manner. Immediately upstream of C targets of plant organelle editing are short *cis*-elements to which the PPR repeats bind [4]. Then a deaminase activity, either present at the C-terminus of the PPR protein (a 'DYW domain') or recruited as a trans-factor, carries out the C-to-U conversion [5–7].

Received: August 30, 2024. Revised: May 2, 2025. Editorial Decision: May 6, 2025. Accepted: May 20, 2025

© The Author(s) 2025. Published by Oxford University Press on behalf of Nucleic Acids Research.

This is an Open Access article distributed under the terms of the Creative Commons Attribution License (<https://creativecommons.org/licenses/by/4.0/>), which permits unrestricted reuse, distribution, and reproduction in any medium, provided the original work is properly cited.

In vascular plants, the PPR proteins studied do not act alone, even if they carry their own deaminase activity. Instead, a complex set of trans-factors interacts with each PPR protein to form a small RNA/protein complex termed the editosome—typically 400 to 600 kD in size [8]. A major question is WHY these accessory factors exist. There are a few known PPR-DYW proteins in a non-vascular plant—a moss—that can perform C-to-U editing without any accessory factors [9]. One hypothesis is that plant accessory factors improve efficiency (percentage of the transcript population that is edited) and/or selectivity (editing only the important C target and not neighboring Cs or distant ones with similar *cis*-elements).

The emerging appeal of PPR proteins as tools for sequence-specific targeting and modification of RNA comes from the deciphering of the code of recognition by which PPR proteins specify their target sequences [10, 11]. Each PPR motif binds to a single ribonucleotide; in each motif, specificity is conveyed by two key amino acid residues in the PPR motif located at the fifth and last position in the motif sequence. The modular nature of PPR proteins, their expansion, and the availability of large sequence databases, combined with the predictability of their interactions with RNA, make it possible to build novel synthetic proteins based on consensus motifs [12]. By utilizing large multiple sequence alignments of natural PPR motifs, the most over-represented amino acids at each position can be determined, while amino acids at position 5 and the last position of the synthetic PPR motif can be chosen according to the PPR-RNA recognition code. The origin of the consensus sequences chosen may vary and different synthetic PPR motif backbones have been produced [12, 13], they all are observed to have superior solubility compared to natural PPR proteins. As a result, synthetic PPR proteins have been easier to express in heterologous systems than natural PPR proteins [12, 13].

The design of a synthetic angiosperm chloroplast editing factor active *in planta* and in *E. coli* [14] allows use of a bacterial system to investigate the role of additional accessory factors. The synthetic PPR protein known as dsn3PLS-DYW was designed with 3 PLS motifs to recognize *rpoA* C-200, which is not edited in *Arabidopsis* homozygous for the *clb19* mutation [15]. A C-terminal DYW domain provides the deaminase catalytic activity. Dsn3PLS-DYW was able to restore a level of editing extent around 45% in the *clb19* mutant plant, but expression in *E. coli* resulted in only about 10% editing of an *rpoA* target sequence. However, co-expression of either the co-factor RIP2/MORF2 or RIP9/MORF9 significantly increased the level of editing to around 35% [14].

RIP2/MORF2 is only one of several accessory factors that are known to affect the efficiency of editing by CLB19 in *Arabidopsis*, according to mutant analysis (Table 1) [16–19]. In this report, we investigated the role of accessory factors, either alone or in combination with each other, in the efficiency of editing of *rpoA*-C200 in *E. coli*. For this purpose, we used the synthetic factor dsn3PLS-DYW after observing that it was much more soluble in bacteria than the natural PPR protein CLB19 (Supplementary Fig. S1). Among the accessory proteins known to affect the editing of the target recognized by CLB19, we focused our investigation on the ones that might still affect the editing of *rpoA* C-200 by the synthetic factor. Unlike the plant CLB19 PPR protein, which requires the trans-factor DYW2 for deaminase activity [20], the synthetic factor possesses a DYW motif at its C-terminus. We therefore excluded from our analysis DYW2 since its presence is no longer required for the editing activity of the synthetic fac-

**Table 1.** *In planta* editing extent of *rpoA*-C200 in mutant or silenced genes encoding accessory proteins

Factors	mutant	wild-type
RIP2 <sup>a</sup>	50%	80%
RIP9 <sup>a</sup>	0%	80%
ORRM1 <sup>b</sup>	26%	81%
OZ1 <sup>c</sup>	0%	71%
ISE2 <sup>d</sup>	41%	88%

<sup>a</sup>reference 16,

<sup>b</sup>reference 17,

<sup>c</sup>reference 18,

<sup>d</sup>reference 19. The comparison was made between cosuppressed leaves and wild-type (wt).

tor (Table 1). Our experiments revealed whether the synthetic PPR protein requires additional accessory proteins in addition to RIP2 and RIP9 in order to carry out editing in bacteria. We tested whether accessory factors affected the affinity of the synthetic PPR protein for its target and demonstrated a correlation of improved affinity with increased editing extent. RNA-seq analysis of bacterial transcriptomes demonstrated that an increase in the efficiency of editing of the target by the accessory proteins was also correlated with an increase in off-target editing.

## Materials and methods

### Bacterial strains

*Escherichia coli* strains used in this study were NEB 10-β competent cells (New England Biolabs, Ipswich, MA, USA, <https://www.neb.com/en-us>) for cloning and Rosetta 2 (DE3) (Novagen) for protein expression and *E. coli* RNA editing experiments.

### Plasmids

Duet vectors (Novagen) pETDuet-1, pCDFDuet-1 and pCOLADuet-1 are T7 promoter bacterial expression vectors designed to co-express two proteins in *E. coli*. These Duet vectors carry compatible replicons and antibiotic resistance markers and may be used together in appropriate host strains to co-express up to six proteins.

### Primers

The primers and oligonucleotides are listed in Supplementary Table S1 and were obtained from Integrated DNA Technologies (IDT, Coralville, IA, USA, <https://www.idtdna.com>)

### Cloning, bacterial expression

The synthetic factor nucleotide sequence was derived from the amino acid sequence published by Royan *et al.* (2021) and the corresponding DNA was synthesized by GenScript (GenScript, New Jersey, USA; <https://www.genscript.com>) and cloned into the *NcoI* and *BamHI* sites of the pETDuet-1 vector. The accessory proteins and CLB19 encoding genes were obtained by PCR reaction with the primers listed in Supplementary Table S1, either directly from *Arabidopsis* genomic DNA (RIP2, RIP9 and CLB19) or after RT-PCR from cDNA (ORRM1, OZ1, ISE2). The transit peptide-encoding sequences were predicted by using TargetP2 (<https://services.healthtech.dtu.dk/services/TargetP-2.0/>) and were removed from all the accessory protein encoding genes and

CLB19. After the PCR reaction the amplicons were cloned into the pCR™8/GW/TOPO vector (Thermo Fisher Scientific, Waltham, MA, USA; <https://www.thermofisher.com>) and the sequences verified to be accurate. Once the sequences were validated, the plasmids were digested with the appropriate restriction enzymes (See *Supplementary Table S1* for details) run on agarose gel and the bands corresponding to the accessory proteins encoding DNA gel-purified and cloned into the expression vectors. The sequence of every expression vector used in this study was checked by whole plasmid sequencing performed by eurofinsgenomics (Louisville, KY, USA; <https://eurofinsgenomics.com>). Bacterial culture followed the protocol of Oldenkott *et al.* (2019); 1 ml samples were harvested, centrifuged at maximum speed for 10 minutes at 4°C, the pellets frozen in liquid nitrogen and stored at -80°C until further use for protein-RNA analysis. The ORRM1 coding sequence (-TP) was cloned into the pMAL-c6T vector (New England Biolabs) by using primers listed in Table S1. The MBP-ORRM1 sequence was then subcloned into the pCDFDuet-1 vector with primers listed in Table S1.

### Protein Extraction

Cell pellets were resuspended in 500 µL of Lysis Buffer (50 mM Tris-HCl, pH 8.0; 1 mM EDTA; 2 mM DTT). Cells were lysed using a 25-second sonication pulse (Heat Systems Ultrasonic Processor W-380, 70% output power, level 5 output control), ensuring complete disruption. Protein concentrations were determined using the Bradford assay (Bio-Rad Catalog #500-0006), with concentrations normalized by diluting samples with Lysis Buffer to match the sample with the lowest protein concentration. Samples were then mixed with an equal volume of 2X Laemmli Buffer (Bio-Rad Catalog #161-0737), gently mixed to avoid frothing, heated in a 95°C water bath for 10 minutes, and then cooled on ice for 2 minutes. Samples were stored at -20°C for short-term and at -80°C for long-term storage.

### SDS-PAGE and Immunoblotting

10 µL of the normalized protein samples were loaded onto a Mini-PROTEAN TGX Any kD (Bio-Rad Catalog #456-9036) SDS-polyacrylamide gel and electrophoresed in 1X SDS-PAGE Running Buffer (25 mM Tris, 192 mM glycine, 0.1% w/v SDS) at 200 V for approximately 35 minutes. After electrophoresis, the gel was rinsed thoroughly with deionized water to remove any residual SDS. The gel was equilibrated in cold 1X Transfer Buffer (25 mM Tris, 192 mM glycine, 20% methanol) for 5 minutes at 4°C prior to transfer. Protein transfer was performed using a nitrocellulose membrane (0.45 µm, Thermo Scientific, REF.88018) in 1X Transfer Buffer using the Trans-Blot Cell (Bio-Rad, Serial No. 49BR32383) at 100 V for 1 hour at 4°C, ensuring the current did not exceed 1.5 A as recommended by the manufacturer. The membrane was dried on clean filter paper at 4°C for 20 minutes to affix the proteins. All subsequent steps were carried out in a black Western blot box (MTC Bio, Cat. No. B1200-7BK) to prevent fluorophore quenching. Blocking was performed at room temperature for 30 minutes using EveryBlot Blocking Buffer (Bio-Rad, Cat. #12 010 020). Primary antibody incubation was carried out overnight at 4°C in a 1:5 000 dilution of the primary antibodies in EveryBlot Blocking Buffer with gentle rocking. The membrane was washed twice with 1X TBST and twice with

1X TBS, each for 5 minutes with moderate rocking. Secondary antibody incubation was conducted at room temperature for 1 hour in a 1:10 000 dilution in EveryBlot Blocking Buffer, followed by two washes in 1X TBST and two in 1X TBS, each for 5 minutes with moderate rocking. The membrane was dried on clean filter paper at room temperature in the dark for at least 20 minutes before imaging. Imaging was performed using the LI-COR Odyssey Imaging System, employing DyLight 700, DyLight 800, and RGB channels for colorimetric ladder visualization. Primary Antibody Mix: (1:5 000): Rabbit anti-Stag pAb (Sino Biological #101290-T38) and Mouse anti-His-tag mAb (GeneScript Cat. No. A00186). Secondary Antibody Mix: (1:10 000): AlexaFluor 488 goat anti-rabbit IgG and AlexaFluor 546 goat anti-mouse IgG or Goat Anti-Mouse IgG (H + L) DyLight 680 Conjugated (Invitrogen REF 35518), Goat anti-Rabbit IgG (H&L) DyLight 800 Secondary Antibody (Invitrogen REF SA535571).

### Ni<sup>2+</sup> Affinity Purification

A 1-L bacterial culture was initiated from a 10 mL fresh pre-culture. Upon reaching an optical density (OD<sub>600</sub>) of 0.4 to 0.7, the culture was cooled on ice for 30 minutes and induced with IPTG to a final concentration of 50 µM. Concurrently, ZnSO<sub>4</sub> was added to a final concentration of 0.4 mM. The culture was then incubated at 16°C for 20 hours. Post incubation, the culture was harvested by centrifugation at 6 000 × g for 30 minutes at 4°C, and the supernatant was discarded. The cell pellet was flash-frozen in liquid nitrogen. The cell pellet was resuspended in a volume ten times its mass of lysis buffer (25 mM Tris-HCl, pH 7.2; 250 mM NaCl; 10% glycerol; 10 mM imidazole; 0.1% NP-40). Lysis was facilitated by the addition of lysozyme to a final concentration of 0.5 mg/mL, followed by 25 sonication pulses of 1 minute each, with 5 minutes of incubation on ice between pulses. The lysate was clarified by centrifugation at 16 639 × g for 30 minutes at 4°C, and the supernatant was then filtered through a 0.22 µm cellulose acetate filter using a vacuum system. The clarified lysate was applied to a 20-mL Econo-Pac polyethylene gravity column containing 1.5 mL of pre-equilibrated HisPur Ni<sup>2+</sup> NTA agarose bead resin (Thermo Scientific, Prod# 88 221) and allowed to bind for 30 minutes. The column was washed five times with 20 mL of wash buffer (25 mM Tris-HCl, pH 7.2, 22°C; 250 mM NaCl; 10% glycerol; 50 mM imidazole). Elution was performed by resuspending the resin in 3 to 5 mL of elution buffer (25 mM Tris-HCl, pH 7.2, 22°C; 250 mM NaCl; 10% glycerol; 200 to 400 mM imidazole) for 20 minutes. Eluted fractions were dialyzed against 500 mL of 20G buffer (25 mM Tris-HCl, pH 7.2, 22°C; 250 mM NaCl; 20% glycerol; 0.5 mM EDTA; 1 mM DTT) for 24 to 36 hours with gentle stirring at 4°C using a Side-A-Lyzer dialysis cassette (Thermo Scientific, Prod# 66 380). The dialyzed protein was concentrated using Amicon 10K and 30K columns (Millipore, Ref. UFC803096; UFC801096) until the final protein concentration reached approximately 1 to 2 mg/mL. The protein was aliquoted, flash-frozen in liquid nitrogen, and stored at -80°C. The efficacy of the purification was assessed via Stain-Free SDS-PAGE using Mini-PROTEAN TGX Stain-Free Gels (Bio-Rad, Cat.# 4 568 126) according to the manufacturer's recommendations. The gels were imaged using the BioRad ChemiDoc MP Imaging System.

## Detection of RNA editing in *E. coli*

Total RNA was extracted from 1 mL of *E. coli* bacterial pellet using the Invitrogen™ PureLink™ RNA Mini Kit (Thermo Fisher Scientific, Waltham, MA, USA; <https://www.thermofisher.com>) according to the manufacturer's instructions. Reverse transcription was performed on DNase-treated total RNA extract using Superscript™ III Reverse Transcriptase (Invitrogen) with the primers listed in [Supplementary Table S1](#) according to the manufacturer's instructions. RT-PCR bulk sequencing of the *rpoA*-C200 target was performed to assay the editing extent. The editing extent was calculated from the electrophoretogram by using BEAT, a python program developed to quantify base editing from Sanger sequencing [21]. For each accessory protein or combination of accessory proteins tested we performed three biological replicates.

## Statistical treatment of bacterial expression experiments

To examine the variability across the outcomes of 46 distinct experiments, each involving three independent measurements from biological replicates, a specific statistical framework was utilized. Analysis of Variance (ANOVA), conducted using the stats package (version 3.6.2) in R, was implemented to evaluate significant differences among the mean values of the experimental groups, revealing significant disparities ( $Pr < 2e-16$ ,  $F = 303.1$ ). Given the significant findings from the ANOVA, Tukey's Honestly Significant Difference (TukeyHSD) test, was also performed with the stats package (version 3.6.2) in R and was subsequently applied for pairwise comparisons among the experimental conditions.

## RNA electromobility shift assays

RNA electrophoretic mobility shift assays (REMSAs) were performed following the protocol of Royan *et al.* (2021). The fluorescence was visualized on an Amersham Typhoon system (GE Healthcare), with a filter for the Cy5 fluorophore and quantified with the analysis toolbox from the ImageQuantTL software version 8.2 (GE Healthcare).

## AlphaFold predictions

For the protein structure predictions of multiple sequences, including those from dsn3PLS-DYW (untagged) and the truncated variants of RIP2 (aa 89–186) and RIP9 (aa 86–192), ColabFold: AlphaFold2 integrated with MMseqs2 was employed [22]. This advanced tool facilitated the generation of highly reliable structural predictions, as indicated by the precision metrics: predicted Local Distance Difference Test (pLDDT) and predicted Template Modeling (pTM) scores, alongside the interface predicted TM score (ipTM) for the complexes of dsn3PLS-DYW with RIP2(89–186) or RIP9(86–192). The accuracy of these predictions is further substantiated by Predicted of Aligned Error (PAE) graphs, provided in the supplementary materials ([Supplementary Fig. S9](#))

dsn3PLS-DYW + RIP2(89–186): pLDDT = 93.1, pTM = 0.885, ipTM = 0.932

dsn3PLS-DYW + RIP9(86–192): pLDDT = 93.1, pTM = 0.878, ipTM = 0.958

To analyze the structural alignment and visualization, the predicted models were superimposed using UCSF Chimera (developed by the Resource for Biocomputing, Visualization, and Informatics at the University of California, San Fran-

cisco, with support from NIH P41-GM103311, [23]), focusing on the chains corresponding to dsn3PLS-DYW. This approach facilitated a detailed comparison between the chains, which were pseudo-colored to enhance differentiation. Visualization of the structures, including the generation of images and movies, was also accomplished using UCSF Chimera, ensuring a comprehensive representation of the structural dynamics and alignments observed.

## Library construction for RNA-seq analysis

Total RNA was extracted from a bacterial pellet from 1 mL of *E. coli* as for the detection of RNA editing. RNA concentration and integrity were assessed using a Qubit 2.0 Fluorometer (Invitrogen) with the Qubit RNA BR Assay Kit (Invitrogen Ref No. Q10211) and an Agilent 2100 Bioanalyzer (Agilent Technologies) with the RNA 6000 Nano Kit (Agilent, Cat No. 5067–1511). RNA libraries were treated with the FastSelect rRNA depletion kit from Qiagen for bacterial depletion (QIAseq FastSelect Epidemiology Kit) and a directional library preparation was done at Cornell RNA Core facility with the NEBNext Ultra II Directional RNA Library Prep Kit for Illumina (New England Biolabs). The libraries were sequenced on an Illumina NovaSeq X instrument with unpaired-end 150 bp reads.

## Quality Control and Read Processing

Raw sequencing reads were assessed using FastQC (v0.12.1) to ensure data quality. Adapter sequences and low-quality bases were removed using Cutadapt (v4.9) in a two-step process: adapters were first removed based on the provided sequences, and then reads were hard-trimmed by 10 nucleotides from both 5' and 3' ends. Quality trimming was applied with a threshold of Q20.

A comprehensive reference genome was constructed by combining the *E. coli* reference genome (NCBI accession number: CP10816.1) with the pETDuet-rpoAC200 plasmid which contains the dsn3PLS-DYW synthetic PPR protein gene and the *rpoAC200* target sequence. The pRARE2 plasmid (included with Rosetta cells and containing rare codon genes and the chloramphenicol resistance cassette) was sequenced and assembled using long-read sequencing services provided by Eurofins Genomics. This plasmid was included in the reference genome for alignment purposes but was excluded from the final off-target analysis due to the absence of appropriate annotations.

## Alignment and BAM File Processing

Sequencing reads were aligned to the constructed reference genome using the BWA-MEM algorithm (bwa-mem2 v2.2.1). Default parameters were applied, including a minimum seed length (-k 19), band width for the banded alignment (-w 100), off-diagonal X-dropoff (-d 100), internal seed search parameter (-r 1.5), clipping penalty (-y 20 and -L 5), minimum chain length discard threshold (-c 500), and scoring metrics including match score (-A 1), mismatch penalty (-B 4), gap open (-O 6), and gap extension (-E 1) penalties, alongside the penalty for unpaired read pairs (-U 17). BWA-MEM's intrinsic soft clipping was utilized to handle read alignments, particularly at read ends where mismatches often occur due to sequencing errors or low-quality.

BAM files generated by BWA-MEM were sorted and indexed using Samtools (v1.18). The samtools calmd function

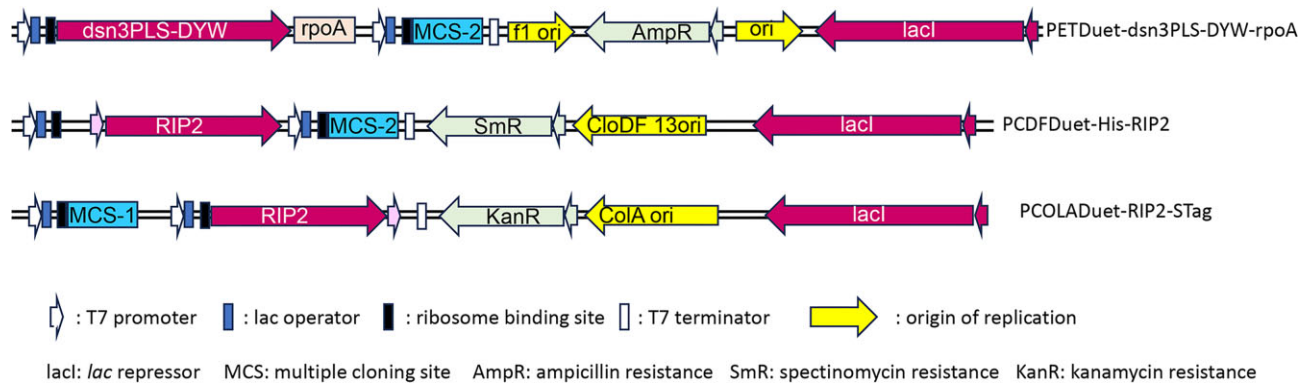


**Figure 1.** Simplified diagram of the vectors used. PETDuet, pCDFDuet, and pCOLADuet are Duet vectors that are designed to allow the co-expression of multiple genes. The Duet vectors are T7 promoter expression vectors, each designed to co-express two proteins in *E. coli*. The Duet vectors carry compatible replicons and antibiotic resistance markers and may be used together in appropriate host strains to co-express up to six proteins. A representation of the vector with the gene it will express is shown, pETDuet with the synthetic factor dsn3PLS-DYW, pCDFDuet, or pCOLADuet with RIP2.

was employed to generate MD tags, preparing the alignments for variant calling with JACUSA2 (v2.0.4) [24]. Technical duplicates were merged before alignment to ensure comprehensive coverage. Quality assurance of alignments was performed with Qualimap (v2.2.1), and HTML reports were generated for each sample.

### Identification of Off-Target RNA Editing Events

Off-target RNA editing events were identified using JACUSA2 (v2.0.4) with parameters optimized for detection accuracy [24]. Call-2 flag was utilized to set comparisons between the RNA samples and the genomic DNA sequences. Libraries were analyzed in a strand-specific manner using the -P RF-FIRSTSTRAND option to maintain correct strand orientation. A base quality filter threshold (-q 20) was applied to exclude bases with a Phred score below 20 and reads with more than two mismatches (-filterNM 2) were excluded to enhance specificity. These settings were chosen to balance sensitivity and specificity, ensuring the identification of true RNA editing events while minimizing false positives.

VCF files generated by JACUSA2 were further analyzed in R (v4.1.1) using custom scripts. The vcfr package (v1.14.0) was used for parsing, followed by stringent filtering criteria. C→T and G→A transitions were selected based on the following: [1] a minimum editing fraction difference of 1% between DNA control and RNA samples, with an error rate limited to 1% of the percentage editing; [2] events supported by read depths above the 1% lower quantile; and [3] a JACUSA2 score threshold above the 95th percentile for samples with editing rates  $\geq 10\%$  and the 98th percentile for samples with editing rates  $< 10\%$ . These criteria ensured the exclusion of SNPs and sequencing errors, focusing on genuine C-to-U RNA editing events.

### Validation and Downstream Analysis

To eliminate sequencing or mapping errors and potential SNPs, we excluded common events between Rosetta samples without PPR or accessory proteins using a custom Python script. FASTA sequences of potential off-targets were extracted using a custom Python program for further analysis with PPRmatcher (<https://github.com/ian-small/PPRmatcher>) and for generat-

ing RNA logos (WebLogo 2.8.2). The PPRmatcher (<https://github.com/ian-small/PPRmatcher>; dsn3PLS.motifs.txt; scoring tables = Kobayashi.tsv) JULIA script was modified to return scores for individual PPR-binding sites, providing granular insights into binding affinities.

Custom Python and R scripts were used to generate RNA heat maps based on the PPRmatcher scores, the RNA logos using WebLogo (<https://github.com/WebLogo/weblogo>), and the comparison tables, offering visual representations of RNA editing events and binding site distributions across all samples.

## Results

### Simultaneous expression of RIP2, RIP9, or ORRM1 with dsn3PLS-DYW in *E. coli*

In order to express the PPR specificity factor along with individual accessory factors, we used the Duet vectors system (Novagen) that was developed to co-express multiple genes in *E. coli*. This system consists of five vectors, each of which is capable of co-expressing two proteins. Maintenance of four plasmids in a single bacterial cell is possible because of compatible replicons and drug resistance genes that these vectors harbor. pETDuet-1 carries the Cole1 replicon and bla gene (ampR) and was used to express the dsn3PLS-DYW, which was synthesized by GenScript (Fig. 1). The *rpoA*-C200 target sequence that we used consisted of 39 nt, 33 nt upstream of the targeted C and 5nt downstream, and was cloned downstream of the dsn3PLS-DYW sequence. Upon transcription, both dsn3PLS-DYW and *rpoA*-C200 are carried on the same transcript. The accessory proteins were cloned in pCDFDuet-1, which carries the CloDF13 replicon and the *aadA* gene (streptomycin/spectinomycin resistance) and in the kanamycin-resistant pCOLADuet-1, which carries the ColA replicon. Each Duet vector has two T7lac promoters, two multiple cloning (MCS) regions, and a single T7 terminator for the cloning and expression of two open reading frames (ORFs). The first MCS encodes an amino-terminal 6-amino acid (aa) His-tag sequence for detection and purification, while the second MCS allows the fusion of an optional carboxy-terminal 15-aa S-tag sequence for detection, purification, and quantification. Each of the 5 accessory proteins known to affect editing extent *in planta*, RIP2, RIP9, ORRM1, OZ1, and ISE2

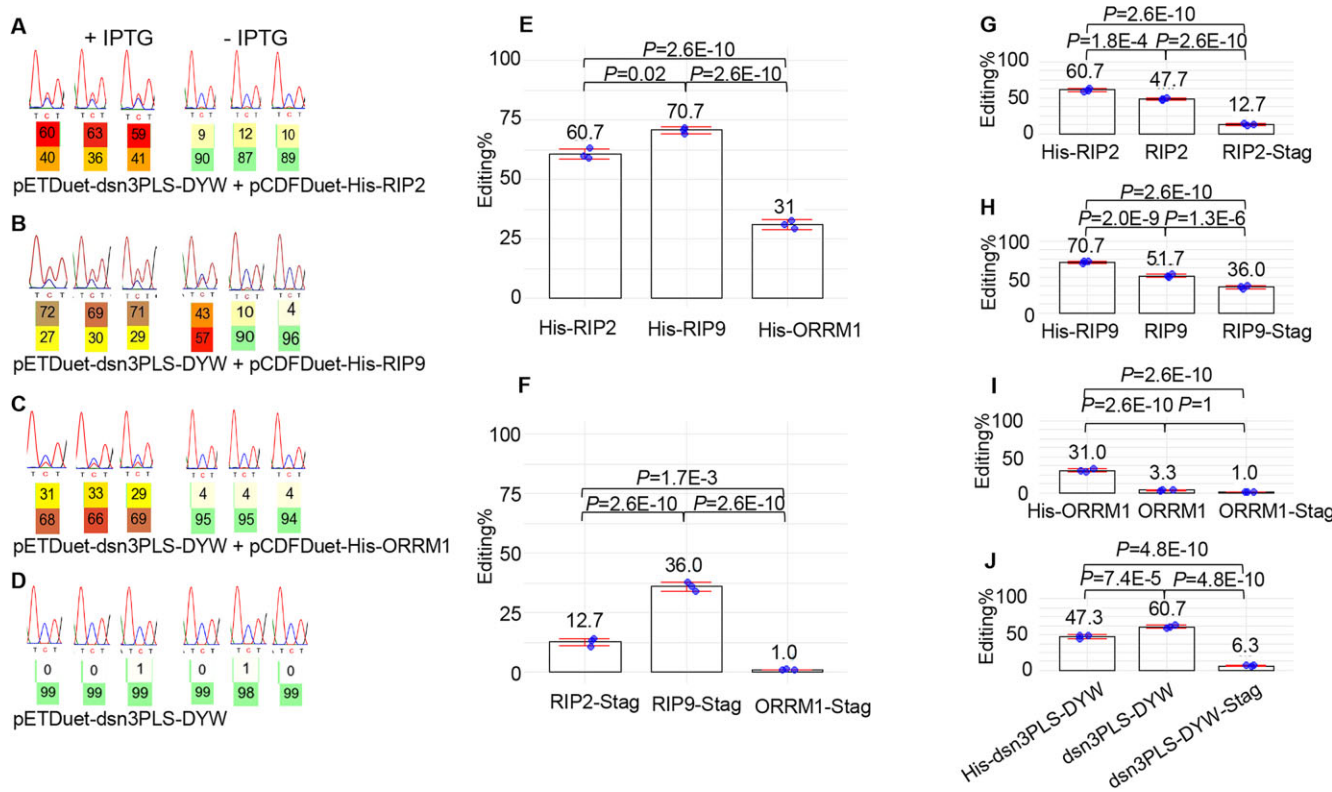


**Figure 2.** The accessory protein RIP9 is the most efficient in increasing the editing extent of *rpoA*-C200 by dns3PLS-DYW in *E. coli*. Left panel, electrophoretogram of RT-PCR bulk sequencing of the *rpoA*-C200 target when the synthetic factor is co-expressed with RIP2 (A), RIP9 (B), ORRM1 (C), or by itself (D). On the left (+IPTG) is the editing observed after induction by IPTG, on the right without induction. The C target is in the middle of the electrophoretogram showing 3 nucleotides T C/T T. Below the targeted C is the percentage of T (upper number) versus C (lower number) as computed by the BEAT software. The expression system is leaky as residual editing extent is observed even in the absence of induction. This residual editing in the absence of IPTG is more pronounced for efficient accessory protein RIP9 than for ORRM1. However, there is absolutely no editing when the synthetic factor is expressed by itself (D). Middle panel, with a tag either at the *N*-terminus (His-Tag) (E) or at the *C*-terminus (S Tag) (F) RIP9 is the most efficient accessory protein to increase the editing extent of the *rpoA*-C200 target. The editing extent of *rpoA*-C200 is given for three biological replicates for each of the accessory proteins. Right panel, RIP2 and ORRM1 are very sensitive to the presence of a tag at their C terminus while RIP9 is less affected. The addition of a tag at the *N*-terminus is beneficiary to the editing function of the accessory proteins, particularly for ORRM1 (I). The editing extent of *rpoA*-C200 is given for three biological replicates in the presence of the synthetic factor and one accessory protein, RIP2 (G), RIP9 (H) or ORRM1 (I). Each of the accessory proteins was expressed using the pCDF-Duet1 vector. His tag is at the *N* terminus of the accessory protein, S tag at the *C* terminus. In J dns3PLS-DYW was co-expressed with pCDF-His-RIP2.

(Table 1) was cloned either in pCDF Duet-1 or pCOLA Duet-1 with a His-N tag, a C-S tag, or no tag (Fig. 1).

Although Royan *et al.* (2021) observed a low level of editing extent (5–10%) when the synthetic dns3PLS-DYW factor was expressed by itself, we did not observe any editing extent in our system by expressing only the PPR editing factor (Fig. 2). This difference could be due to our use of a different expression vector (pETM20 versus pETDuet-1) and thus a possible difference in the level of expression of the synthetic factor.

When we expressed the synthetic PPR editing factor with RIP2, we observed approximately 60% editing, while RIP9 conferred 70% editing (Fig. 2A and B). In contrast, Royan *et al.* (2021) observed only 35% editing. The level of editing extent of *rpoA*-C200 in our experiments was around 30% when the synthetic factor was co-expressed with ORRM1 (Fig. 2C). These results were obtained with a His-tag attached at the *N* terminus of the accessory proteins (Fig. 2E). We also tested these accessory proteins in a different configuration, with an S-tag attached at their *C* terminus (Fig. 2F). Again, RIP9 was the most efficient accessory protein in increasing the editing extent of the *rpoA*-C200 target in the presence of the

synthetic factor. However, the presence of a tag at the *C* terminus was detrimental to the function of the accessory proteins, as they all showed a significant reduction in their effect on the editing extent of the target. In the case of ORRM1, there was a complete obliteration of its function, with an editing extent that was close to zero (Fig. 2F). Given their small sizes, 6 aa for the His-tag and 15 aa for the S-tag, the effect is likely caused by the position of the tag disrupting protein function.

Based on this observation, we tested the function of these three accessory proteins in the absence of any tag (Fig. 2G–I). Surprisingly, a His-tag at the *N* terminus results in a higher editing extent for all the accessory proteins when compared to an absence of tag, possibly due to an increase in the stability of these proteins. This observation is particularly true for ORRM1 which, when deprived of a His-tag at the *N*-terminus, experienced a severe reduction in the editing extent (3% versus 31%) of the target when co-expressed with dns3PLS-DYW (Fig. 2I). The absence of an antibody against the Arabidopsis ORRM1 did not allow us to test whether the addition of His tag at the *N*-terminus affects the stability of this protein. Furthermore, we tested the position of the tag on

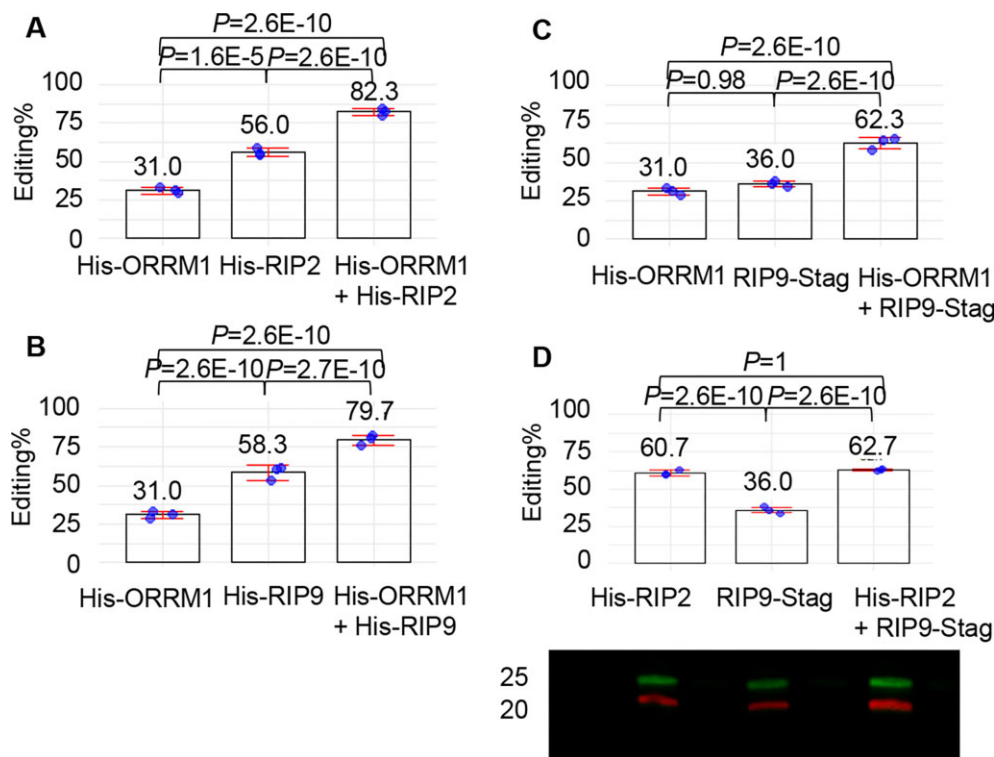


**Figure 3.** ORRM1 and RIP2 (RIP9) have an additive effect on the editing extent of the *rpoA*-C200 target. **(A)** Editing extent of the *rpoA*-C200 by dsn3PLS-DYW in the presence of ORRM1 (left), RIP2 (middle) or both ORRM1 and RIP2 (right). **(B)** and **(C)** Editing extent of the *rpoA*-C200 by dsn3PLS-DYW in the presence of ORRM1 (left), RIP9 (middle) or both ORRM1 and RIP9 (right). ORRM1 was expressed in pCDF-Duet1 with a His-tag, and RIP2 and RIP9 were expressed in pCOLA-Duet1 **(A and B)**. **(C and D)** RIP2 and RIP9 were expressed in pCDF-Duet1. Below the graph is shown a Western blot demonstrating that both RIP2 (lower band) and RIP9 (upper band) are expressed in the three biological replicates (on the left are indicated a marker size in kDa). The editing extent of *rpoA*-C200 is given for three biological replicates.

the function of the synthetic factor itself. Unlike the accessory proteins, a His-tag at the N-terminus of the dsn3PLS-DYW reduces the editing extent of the target when co-expressed with RIP2 (Fig. 2J). Similarly to the accessory proteins, the addition of a S tag at the C-terminus of the synthetic factor is very detrimental to its function, as the level of editing extent in the presence of RIP2 is severely reduced (Fig. 2J).

Even though pCDF-Duet1 and pCOLA-Duet1 are supposed to have the same copy number (20-40) according to the Novagen user protocol, our experience in isolating these plasmids has generally been a low yield for pCOLA-Duet1. The lower copy number is reflected in a reduction of the expression of the accessory proteins in pCOLA-Duet1 when compared to pCDF-Duet1. The lower copy number and expression levels can affect the level of editing extent for certain accessory proteins in certain configurations, but not in others. For instance, a strain expressing ORRM1 with a His-tag experiences a reduction of almost half of the editing extent (17% versus 31%) depending on the expression vector used (pCOLA-Duet1 versus pCDF-Duet1), respectively (Supplementary Fig. S2). A similar reduction occurs when RIP9 has either a His- or an S-tag, 71% versus 58% of editing when expressed in pCDF-Duet1 versus pCOLA-Duet1, or 36% versus 11%, respectively (Supplementary Fig. S2). However, a strain expressing RIP2 with a His tag is not affected by the choice of expression vector; either results in a similar level of editing extent.

Although both OZ1 and ISE2 affect editing of *rpoA*-C200 in plant, neither of them affected editing when co-expressed by themselves with the synthetic factor (Supplementary Fig. S3).

#### ORRM1 and RIP2 (RIP9) act additively to contribute to the editing of *rpoA*-C200 by dsn-3PLS-DYW

In order to probe the role of ORRM1 in the presence of either RIP2 and RIP9, we tested the three combinations of two accessory proteins, RIP2 + RIP9, ORRM1 + RIP9, and ORRM1 + RIP2. Of these, ORRM1 + RIP2 or ORRM1 + RIP9 showed a very significant increase of the *rpoA*-C200 editing extent when compared to the individual contribution of each accessory protein (Fig. 3). The editing extent in the presence of RIP2 and ORRM1 is almost the summation of each individual effect (82% versus 31% + 56%), suggesting that RIP2 and ORRM1 are acting in independent ways to allow the editing of *rpoA*-C200 by the synthetic factor (Fig. 3A). A similar observation can be made for the combined effect of ORRM1 and RIP9 (Fig. 3B and C). The editing extent in the presence of both ORRM1 and RIP9 is almost the summation of their individual effects. In Fig. 3B, RIP9 is expressed in pCOLA-Duet1, which results in a lower editing extent of the *rpoA*-C200 target than when expressed in pCDF-Duet1 (Supplementary Fig. S2). We tested RIP9 in both configurations with either a N-His tag (Fig. 3B) or a C-S tag (Fig. 3C): both experiments lead to the same conclusion about the cumulative effect of RIP9 and ORRM1 when they are co-expressed.

In contrast, RIP2 and RIP9 do not show any sign of co-operation when they are co-expressed in the presence of the synthetic factor (Fig. 3D). The level of editing extent of the target is not significantly different in the presence of RIP2 and RIP9 (63%) from the editing extent when only RIP2 is present (61%).

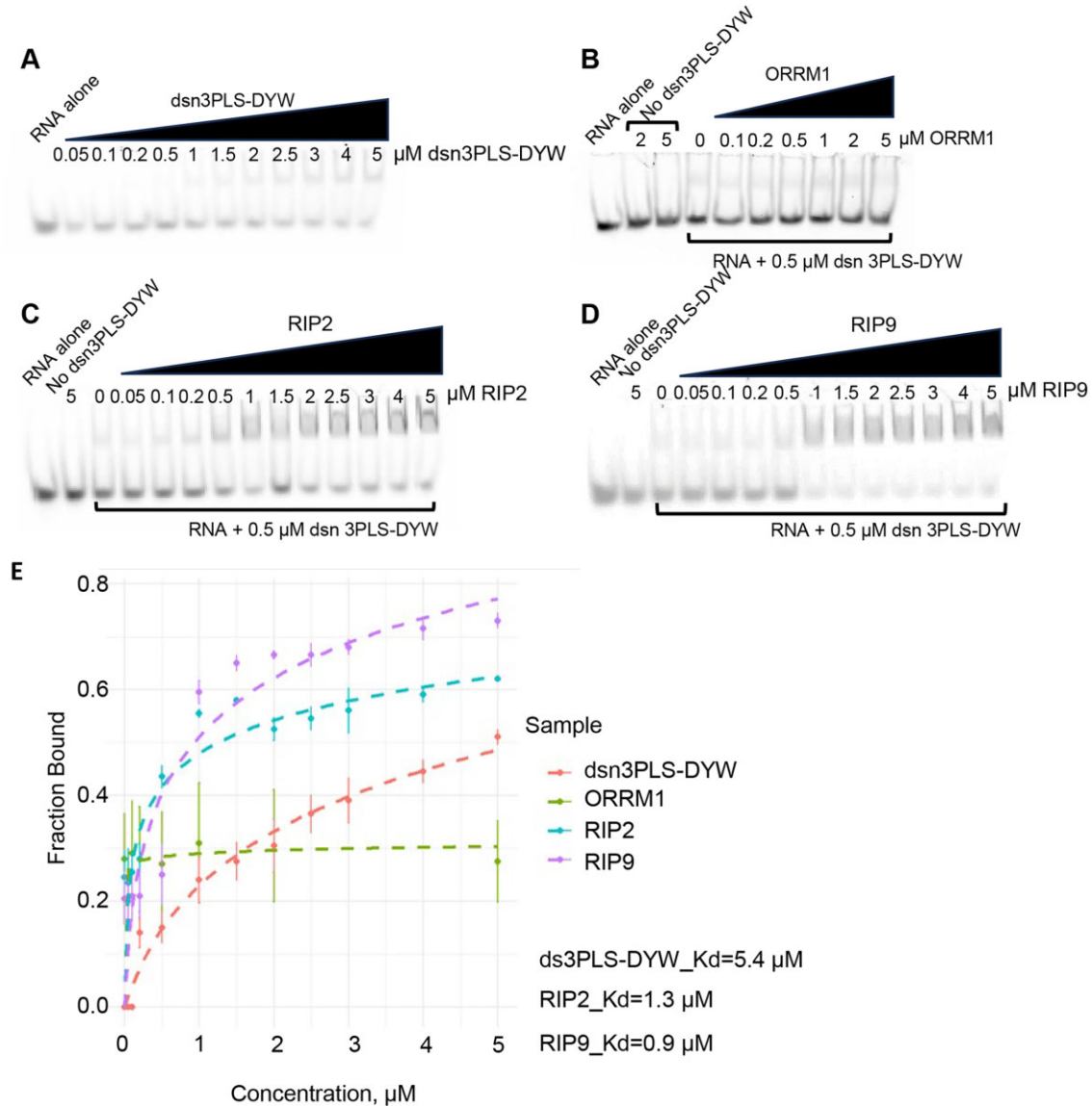


**Figure 4.** RIP2 and RIP9 but not ORRM1 increase the binding affinity of dsn3PLS-DYW protein for its RNA ligand. Gel shift assays were performed with dsn3PLS-DYW alone (A), or dsn3PLS-DYW in the presence of an increasing amount of ORRM1 (B), RIP2 (C) or RIP9 (D). RIP2 and RIP9 do not bind the RNA target by themselves (No dsn3PLS-DYW lane in C and D). (E) Fraction bound in each gel shift assay was plotted against the concentration of the accessory protein. Each reaction was duplicated. A logarithmic fitting model allowed to estimate the Kd for dsn3PLS-DYW and RIP2 and RIP9 with dsn3PLS-DYW.

#### Co-expression of OZ1 or ISE2 with RIP2 does not increase editing efficiency

As described above, OZ1 and ISE2 do not affect the editing extent of the target when they are co-expressed with the synthetic factor (Supplementary Fig. S3). In order to determine the roles of OZ1 and ISE2 in editing of *rpoA*-C200, we co-expressed each one in the presence of RIP2 and the synthetic PPR editing factor. The editing of the target is reduced when OZ1 with a His tag is co-expressed with RIP2 when compared to RIP2 alone (52% versus 61%, Supplementary Fig. S4A), indicating an inhibitory effect of His-OZ1. Therefore, we co-expressed RIP2 and OZ1 without a tag and found that the editing extent was slightly increased when compared to RIP2 alone (65% versus 56%, Supplementary Fig. S4B). Both the inhibitory and stimulatory effects exhibit a *P* value of 0.08.

RIP2 and RIP9 increase the affinity of the synthetic factor for its RNA ligand, while ORRM1 increases the affinity only when combined with another accessory protein

How do the accessory proteins increase the editing efficiency of the synthetic dsn3PLS-DYW factor for its target in bacteria? The RNA binding activity of a designer PLS-type PPR protein was reported to be drastically increased on RIP9 (also referred to as MORF9) binding via conformational changes of the PPR protein [25]. We used gel-shift assays to determine whether RIP2, RIP9, or ORRM1 could increase the affinity of dsn3PLS-DYW for its target. Dsn3PLS-DYW was cloned in the expression vector PETM20 and was fused at its N-terminus with thioredoxin (109aa) followed by a 6xHis tag. As a result, the recombinant dsn3PLS-DYW carried a 133 aa tag at its N-terminus (Supplementary Fig. S5). RIP2, RIP9 and ORRM1

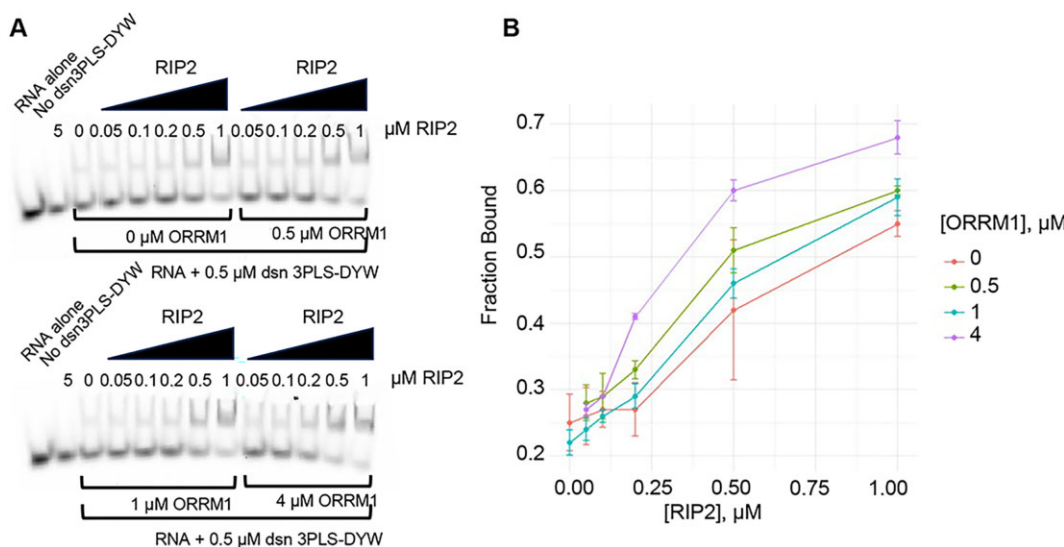


**Figure 5.** ORRM1 in the presence of RIP2 enhances the binding affinity of dsn3PLS-DYW protein for its RNA ligand. **(A)** Gel shift assays were performed with dsn3PLS-DYW in the presence of an increasing amount of RIP2 and a constant amount of ORRM1 : 0  $\mu$ M (left upper gel), 0.5  $\mu$ M (right upper gel), 1  $\mu$ M (left lower gel), and 4  $\mu$ M (right, lower gel). RIP2 does not bind the RNA target by itself (No dsn3PLS-DYW lane). **(B)** Fraction bound in each gel shift assay was plotted against the concentration of RIP2. Each reaction was duplicated. The fraction bound is more important for the higher amount of ORRM1 (4  $\mu$ M, upper curve).

were expressed from the pCDF-Duet1 vector with a His tag. We increased the length of the tag to 10 x His for RIP2 to improve its purification. Each recombinant protein was purified from overnight IPTG-induced cultures using Ni<sup>2+</sup> + affinity purification (Supplementary Fig. S6).

The synthetic PPR editing factor can shift the RNA target, but with limited efficiency (Fig. 4A). We then tested ORRM1, RIP2, or RIP9 by adding an increasing amount of the accessory protein in the presence of a constant amount of the synthetic factor and the RNA target. No increase in the amount of the higher molecular mass complex was observed with ORRM1, demonstrating that ORRM1 has no effect on the RNA binding activity of the synthetic factor (Fig. 4B). In contrast, there was a very noticeable increase in the complex when we repeated this experiment with RIP2 (Fig. 4C) or RIP9 (Fig. 4D). Both proteins are not able to bind the RNA target (no dsn3PLS-DYW lane in Fig. 4C and D) by themselves, confirming that their effects are mediated by binding to the synthetic factor. The experiments presented in Fig. 4 were repeated and the intensity of the lower band (unbound) and the upper band (bound) were quantified for each lane. Binding was estimated by plotting the fraction bound against the concentration of the accessory protein (Fig. 4E). The estimated Kd for the synthetic factor was significantly reduced by the addition of RIP2 or RIP9. The enhancement of the RNA binding activity was more prominent with RIP9 than with RIP2 (Fig. 4E).

Given that ORRM1, when co-expressed in bacteria with either RIP2 or RIP9, increases the editing efficiency of the target (Fig. 3), we tested whether the enhanced binding activity of the synthetic factor by RIP2 could be influenced by the presence of ORRM1. Gel-shift assays were performed with an increasing amount of RIP2, but with a constant amount of ORRM1. The amount of ORRM1 was serially increased from 0  $\mu$ M to 4  $\mu$ M (Fig. 5A). The highest amount of ORRM1 tested (4  $\mu$ M) resulted in a larger fraction bound than in the absence of ORRM1, particularly for the points corresponding to 0.2, 0.5, and 1  $\mu$ M of RIP2 (compare purple and orange curve in Fig. 5B). The affinity curve obtained with intermediate amounts of

ORRM1 (0.5 and 1  $\mu$ M) were between the ones obtained with 0 and 4  $\mu$ M (Fig. 5B). Therefore, this experiment demonstrates that ORRM1 has a positive effect on the enhanced binding activity of the synthetic factor mediated by RIP2.

#### RNA-seq analysis identifies 34 off-targets in the bacterial transcriptome

RNA-seq was performed on 14 bacterial RNA samples, 11 samples from bacteria expressing the synthetic factor with various combinations of accessory proteins, and 3 control samples: bacteria expressing the synthetic factor alone and bacteria not transformed, induced or not induced with IPTG (Supplementary Table S2). Editing of the target was identified in the 12 samples expressing the synthetic factor with its target. Editing of the target was 4.5% in the sample expressing only the synthetic factor, while no editing was detected by the less sensitive method of RT-PCR bulk sequencing (Fig. 2D). Among the 12 samples expressing the synthetic factor, four did not show any off-target editing. In addition to the bacteria expressing only the synthetic factor, samples expressing ORRM1 (either with pCDF or pCOLA) and ORRM1 in the presence of ISE2 did not exhibit any off-target editing. The number of off-target editing events ranges from 4 to a maximum of 19, which was observed for sample 6, which co-expresses the synthetic factor with ORRM1 and RIP2 (Fig. 6A). We detected off-target editing for eight samples, for which the logo of the sequences 15 nt upstream and 1 nt downstream of the edited C is given in Fig. 6B.

Several positions in the sequence of off-targets deviate from the expected predicted nucleotide based on the recognition code. These positions are highlighted in purple in Fig. 6A. The most deviant position is found at -8 where a U is expected to be found but where predominantly a G is found in 15 of the 18 off-target sequences (Fig. 6A). This bias occurs in all the samples analyzed as reflected by the logo sequence obtained for each of them and across all samples (Fig. 6B). The next position to diverge significantly from the expectation based

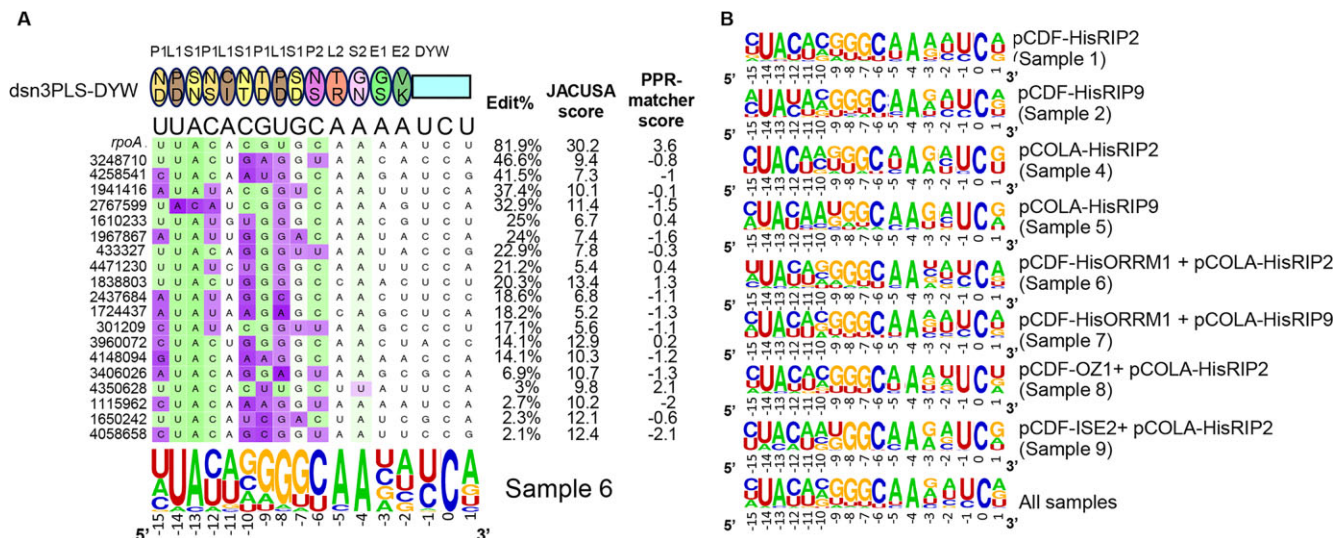


**Figure 6.** Identification of off targets reveals several positions in their sequences that deviate from the PPR recognition code. **(A)** Alignment of the synthetic editing factor with the sites edited in the bacterial transcriptome of Rosetta co-expressing dsn3PLS-DYW, the synthetic factor and the *rpoA* target (pETDuet) with ORRM1 (pCDF) and RIP2 (pCOLA). The dsn3PLS-DYW protein is represented by a model with oval for each PPR motif including the 5<sup>th</sup> (upper aa) and last (lower aa) specificity-determining amino acids. Below the protein model is the sequence of the *rpoA* target site. The coordinates of each off-target site on the bacterial chromosome are given on the left. The target sites are colored according to the PPR matcher score at each position, from favored (green) to neutral (white) to disfavored (purple). The percentage of edited transcripts at each site is indicated on the right and calculated from the RNA-seq analysis (see Materials and methods for details). The JACUSA score reflects the confidence of a true editing event (the higher, the more confidence, see materials and methods for the threshold used). The PPR matcher score is a metric that indicates how well the sequence fits the PPR recognition model. The sequence logo indicates the nucleotide biases at each position and were computed with WebLogo excluding the *rpoA* target sequence and weighing each sequence with editing extent. **(B)** Sequence logos representing the consensus of off-targets for each sample. Like in **(A)** the *rpoA* target sequence was excluded and the sequences were weighed with editing extent. The logo at the bottom represents the consensus sequence of off-targets found across all samples.

on the recognition code across all samples is -15, where a C is predominantly observed instead of a U in 6 of the 8 samples (Fig. 6B, bottom logo). These two positions, -15 and -8, are the only ones that deviate consistently across all samples and show the same bias towards C and G, respectively (Fig. 6B, bottom logo). Other positions exhibiting a different nucleotide in the consensus logo for some samples but not across all samples are -10, -9, and -12. At -10, 4 samples show a nucleotide different from the expected C including the sample analyzed in Fig. 6A where a G is observed in 8 of the 15 off-targets. However, this bias toward G at position -10 is not observed across all samples as reflected by the presence of a C in the logo obtained for all samples (Fig. 6B, bottom logo). At positions -9 and -12 two samples and one sample show in their logo sequence a nucleotide different from the expected one, respectively (Fig. 6B).

It is noteworthy that the most deviant positions in the off-target sequences are observed where a pyrimidine is located, U at -15 and -8 and C at -10. The predictive value of the PPR matcher score for the level of editing extent of the off-targets is rather poor, as illustrated by the low level of editing, 3%, of the site located at 4 350 628, which has the highest score, 2.1, among the off-targets observed for sample 6, which co-expresses the synthetic factor with ORRM1 and RIP2 (Fig. 6A). A significant, albeit weak, correlation ( $R^2 = 0.12$ ) between the editing extent of the off-targets and the PPR matcher score was only found for sample 1, which co-expresses the synthetic factor with pCDF-RIP2. Although the recognition code predicts a neutral or slightly favored nucleotide at position -5 and -4, respectively, we observed a very strong bias toward A at both positions in all the samples analyzed (Fig. 6).

The total number of different off-targets found across the 8 samples amounts to 34 (Table 2). Among those, 16 are uniquely found in one sample while four are found in two samples, six in three samples, three in four samples, one in five samples, two in six samples and two in eight samples. The confidence in true editing events for off-targets is higher for the 18 sites that have been detected in more than one sample. However, we feel confident that even events detected in only one sample are true positive events for most of them because our threshold of detection is rather conservative (see Materials and Methods for details on our screening). Furthermore, their sequences generally fit the consensus logo defined across all samples. For example, the site 4 471 230, which is uniquely detected in sample 6, which co-expresses dsn3PLS-DYW with ORRM1 and RIP2 (Table 2), has a recognition sequence very similar to the consensus logo across all samples (Fig. 6). The only noticeable discrepancy concerns the position -10 where a U is located in the sequence of the 4 471 230 site. There is no strong relationship between the level of editing extent of the off-targets and their detection in more than one sample ( $R^2 = 0.3$ ). As an example, sites 433 327 and 4 471 230 are edited at 22.9% and 21.2%, respectively, but are unique to sample 6 (Fig. 6A, Table 2). Inversely, site 4 350 628 is detected in samples 2, 6, and 7 with a level of editing extent of 1.8%, 3%, and 2.9%, respectively (Table 2). This result comes from the contribution, in addition to the editing extent, of the JACUSA score, which depends on the quality of the reads and the depth of the coverage in the screening of the off-target events.

Among the 34 off-target editing events, 21 occur in the annotated strand of coding sequence and result in an amino acid change (Supplementary Table S3). The highest edited off-

**Table 2.** Editing extent of the *rpoA* target and the off-target sites in the bacterial samples analyzed

sites <sup>a</sup>	sample1 <sup>b</sup>	sample2	sample3	sample4	sample5	sample6	sample7	sample8	sample9	sample10	sample11	sample14	#samples <sup>c</sup>
<i>rpoA</i>	<b>62.31<sup>d</sup></b>	71.0	30.2	57.3	59.1	81.9	78.5	68.0	58.1	22.7	15.6	4.5	12
301 209	<b>10.4</b>	17.8		7.6		17.1	12.3	21.9					4
433 327	5.4					22.9							1
779 169	<b>10.7</b>												1
846 395	1.2	0.7		0.2		1.1		0.9					1
957 341	0.4	1.0		0.4	0.2	0.9	0.4	1.3					1
998 460	5.2				<b>10.9</b>	3.2							1
1 115 962	0.8	<b>1.1</b>		0.7	0.5	2.7	1.1	1.6	0.6				2
1 610 233	3.8					25.0		17.5					2
1 650 242						2.3	0.6						1
1 724 437	6.5	13.7			<b>14.8</b>	18.2							3
1 821 466	<b>38.5</b>	14.9		10.9		25.0	28.0	46.7	20.0				5
1 838 803	<b>14.6</b>	10.1	0.9	6.8	6.0	20.3	11.1	18.3	9.4		0.4		8
1 941 416	16.8	21.8		6.0	14.3	37.4	26.6	33.9	9.3				6
1 967 867		10.8				24.0	14.7						3
2 437 684	4.4	14.0				<b>18.6</b>	11.3						3
2 469 966	5.3					7.5							1
2 728 082	6.1	2.2		5.0		1.3	0.8	0.9					3
2 728 396	0.8	1.5	0.8	0.8	1.6	2.0	2.0	2.0	1.0	1.0	0.6	0.1	1
2 767 599	7.5	6.0		5.7	2.4	32.9	12.5	13.4	10.1				6
3 018 155	1.8	13.2											1
3 146 210	<b>2.1</b>	1.4		1.0	0.5	1.3	0.3	1.4	0.6				1
3 248 710	<b>11.1</b>	3.5		5.3	4.2	<b>46.6</b>	<b>18.2</b>	9.1	5.7				3
3 406 026	1.8	1.5		1.0	0.9	<b>6.9</b>	2.3	2.6	1.0				1
3 960 072	3.7	3.4		1.4	1.8	<b>14.1</b>	8.7	4.1	2.7				2
4 036 064	0.6	<b>1.4</b>		0.5	0.7	1.1	0.5	1.2	0.6	0.3			1
4 058 658	<b>1.4</b>	0.6		0.8	0.4	<b>2.1</b>	0.6	2.0	<b>1.1</b>				4
4 118 470		9.7											1
4 145 999	1.0	1.5		0.8	0.4	0.7	0.4	1.2	0.4				1
4 148 094	7.3	5.1		4.7	3.7	<b>14.1</b>	8.2	8.1	3.2	0.9	1.0		4
4 258 541	<b>38.1</b>	41.6		<b>16.5</b>	<b>46.8</b>	41.5	45.2	<b>45.7</b>	23.2				8
4 289 975	<b>10.0</b>					21.9							1
4 350 628	0.6	1.8		0.4	0.2	3.0	2.9	0.3					3
4 471 230							<b>21.2</b>						1
4 495 686	<b>5.8</b>	5.4		2.6	4.9	7.1	7.4	4.4					2

<sup>a</sup>sites are denominated by their coordinates on the bacterial chromosome.<sup>b</sup>sample identification is explained in [Supplementary Table S2](#).<sup>c</sup>number of samples where the site was above the significant threshold for detection.<sup>d</sup>number in bold denote sites that passed the significant threshold.

target (21%), which results in a proline to leucine substitution, occurs in a hydroxyphenyl acetate permease. Interestingly, the two highest edited off-targets, 4 258 541 (37%) and 1 821 466 (26%), occur in the opposite strand to the annotated one. Because the bacterial genome is rather compact, these events might actually be taking place in the 5' or 3' UTRs of adjacent genes. We confirmed the existence of these two events by bulk-sequencing of RT-PCR products ([Supplementary Fig. S7](#)). We chose two different samples to assay the level of editing extent of the two off-targets, sample1 (dsn3PLS-DYW + pCDF-RIP2) for 4 258 541 and sample 2 (dsn3PLS-DYW + pCDF-RIP9) for 1821466. Both samples show detectable level of editing with the 4 258 541 level of editing slightly lower (26% versus 38%) when compared to RNA-seq analysis, while 1 821 466 editing was slightly higher (20% versus 15%) when compared to RNA-seq analysis ([Supplementary Fig. S7, Supplementary Table S3](#)).

One of the pressing questions about the function of the accessory proteins in editing is their effect on efficiency (editing extent of the target) and/or selectivity (the amount of off-target editing) and if it was possible to disentangle them. We observed that the number of off-targets detected in each bacterial transcriptome assayed is strongly dependent on the level of editing extent of the *rpoA* target (Fig. 7). The most efficient combination of accessory proteins, pCDF-HisORRM1 + pCOLA-HisRIP2, which results in 82% editing of the *rpoA*-C200 target is also exhibiting the highest number of off-targets (19 off-targets, Fig. 6A).

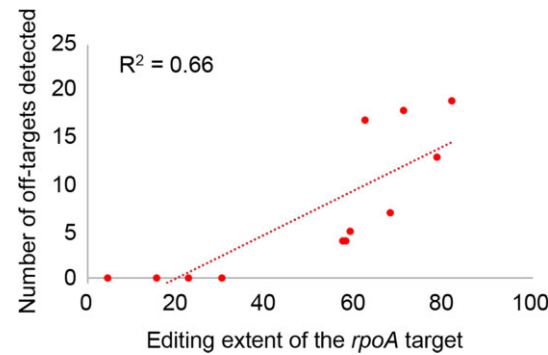


**Figure 7.** The number of off-targets detected in the bacterial transcriptome depends on the editing extent of the *rpoA* target. The level of editing extent of the *rpoA* target is a reflection of the efficiency of the editosome. The more efficient the editosome, the higher number of off-targets.

## Discussion

We have expressed a synthetic factor in a heterologous system to determine whether accessory proteins that are required for efficient editing by the endogenous PPR protein are also important for editosome function in *E. coli*. C to U editing does not naturally occur in *E. coli*, ensuring that only Arabidopsis proteins heterologously expressed could participate into the editing of the target. The choice of a synthetic editing factor, dsn3PLS-DYW, has been dictated by its improved solubility in

bacteria compared to its natural counterpart, CLB19. More importantly, dsn3PLS-DYW has been shown to complement the editing defect in *clb19* mutant plants [20], warranting that the synthetic factor is able to integrate a functional editosome *in planta*. Mutational analysis has identified several accessory proteins likely to be components of the natural CLB19 editosome [16–19]. We decided to investigate the involvement of these candidate accessory proteins in their contribution to the editing of the *rpoA* target by dsn3PLS-DYW in *E. coli*.

Except for RIP/MORF9 protein, for which structure in complex with a PPR editing factor has been obtained [25], there is little known about additional accessory proteins that affect editing extent *in planta* in corresponding mutants. The RIP/MORFs and ORRMs are common to chloroplasts and mitochondria, while OZ1 is specific to the chloroplast [16–18, 26–29]. We have taken three approaches to investigate the contribution of these accessory proteins in the editing process. Bacterial co-expression in the presence of the synthetic dsn3PLS-DYW PPR protein and the RNA target allowed us to test whether these proteins, either individually or in combination could influence the level of editing extent of the target. REMSAs were used to measure the influence of the accessory proteins on the RNA binding activity of the synthetic factor. RNA-seq analysis of the bacterial transcriptomes of the different samples co-expressing the synthetic factor with various combinations of accessory proteins identified 34 off-targeting events. Investigation of their upstream sequences revealed not only positions in agreement but also positions that diverge significantly from the PPR code.

Like Royan *et al.* (2021), we observed a positive contribution of RIP2 and RIP9 to the editing extent of the *rpoA*-C200 target by dsn3PLS-DYW in *E. coli*. However, the level of editing was significantly higher in our co-expression experiments. 61% for strains expressing RIP2 and 71% for RIP9 versus 35% (Fig. 2). Several possibilities can explain this discrepancy: a different expression vector (pCDFDuet-1 versus pETM11), a shorter version of RIP2 and RIP9 in the previous experiment, 48 aa (22 at N-terminus and 26 at the C-terminus) and 51 aa (15 at N-terminus and 36 at the C-terminus), respectively. These differences are significant, as RIP2 and RIP9 are relatively small proteins, so that the RIP/MORF proteins in Royan *et al.*'s (2021) experiments lack ~30% of the proteins' compositions. In addition, in their experiments, one and two cysteines were mutated to serine, for RIP2 and RIP9, respectively, presumably to avoid the formation of disulfide bonds. We found that RIP9 contributes more to editing efficiency than RIP2 in two of the configurations we tested, with a tag either at the *N*- or the *C*-terminus.

We found that ORRM1, which had not previously been expressed in *E. coli* with a PPR editing factor and plant editing target, can result in around 30% editing of the RNA target. ORRM1 was originally identified by its homology to the RIP/MORF family [17]. ORRM1 is an essential plastid editing factor; in Arabidopsis and maize mutants, RNA editing is impaired at particular sites, with an almost complete loss of editing for 12 sites in Arabidopsis and 9 sites in maize. The level of editing extent of *rpoA*-C200 in the Arabidopsis *orm1* mutant is 26%. Therefore, ORRM1 is not essential to the editing of this site *in planta*, though its presence improves editing efficiency.

In contrast, OZ1 is essential to the editing of *rpoA*-C200 because editing is completely absent in the *oz1* mutant plant [18]. Furthermore, although OZ1 has not been formally

shown to interact with CLB19, these two proteins likely interact since OZ1 interacts with other components of the editing complex, such as OTP82 and CRR28, which are other PPR recognition factors [18]. Therefore, we were surprised that we detected no effect of OZ1 in the bacterial expression system. One explanation may be that we predicted an incorrect transit sequence of 79aa, and perhaps the genuine sequence is shorter so that some important *N*-terminal sequence was absent in our expressed protein. Alternatively, the lack of activity of OZ1 in the bacterial expression system might be a lack of required post-translational modifications (PTMs) or improper folding in *E. coli*.

The lack of effect of ISE2 in the bacterial expression system may be due to its lower importance in *rpoA*-C200 editing. ISE2 is a chloroplast-localized RNA helicase that is required for multiple chloroplast RNA processing steps including RNA editing, splicing and processing of chloroplast ribosomal RNAs [19]. The editing extent of *rpoA*-C200 is reduced to ca 40% in co-suppressed leaves (chlorotic tissues of mutant *ise2* plants expressing a 35S:ISE2–GFP transgene). Thus, ISE2 is not essential to the editing of *rpoA*-C200 *in planta*.

The co-expression of ORRM1 with RIP2 or RIP9 in the presence of the synthetic factor resulted in an editing extent of ~80%, which is higher than the level of editing extent, around 45%, achieved by the synthetic factor when introduced into *clb19* mutant plants [14]. The higher efficiency of editing in bacteria is likely due to a high expression of both the synthetic factor and the accessory proteins. In contrast, the expression of these editing factors *in planta* might be a limiting factor. The Arabidopsis CLB19 native promoter and 5' untranslated region (consisting of the 1 kb of DNA sequence from upstream of the start codon) was used to drive expression of the synthetic factor transgene in *clb19* mutant plants [14]. It is known that native PPR promoters are generally weak [1], moreover, only three plants were analyzed in the work by Royan *et al.* [14]. It is possible that if they had screened more transgenic events, they might have identified plants with a higher editing extent of the *rpoA*-C200 target. The cumulative effect of ORRM1 with either RIP2 or RIP9 is almost perfectly additive, suggesting that their involvement in the editing process is independent from each other. By contrast, RIP2 and RIP9 are redundant since their co-expression did not improve the editing extent of the target. This result is not really surprising since RIP2 and RIP9 are highly similar (60% identity, 74% similarity at the aa level). Furthermore, an AlphaFold prediction of dsn3PLS-DYW complexed with RIP2 or RIP9 shows a perfect alignment of these two latter proteins, suggesting that they bind the synthetic factor in a very similar way (Supplementary Fig. S8A, B, C).

The gel shift assays indicate that the effects of RIP2 and RIP9 on the editing process are mediated by an interaction between these proteins and the PPR recognition factor that results in an enhanced binding activity of the factor for its RNA ligand. This increased RNA binding results from conformational change of the synthetic factor upon binding RIP9 [25]. Our experiments also demonstrate that the editing efficiency in the bacterial expression system correlates with the RNA binding activity of the synthetic factor triggered by the accessory protein or the combination of them. For instance, RIP9 is significantly more efficient than RIP2 in editing of *rpoA*-C200 in bacteria in the presence of dsn3PLS-DYW (71% versus 61%). In REMSA, RIP9 also resulted in more protein complexed with RNA or smaller Kd, reflecting a better RNA bind-

ing activity of the synthetic factor for its RNA target (Fig. 4). A closeup of the AlphaFold prediction of dsn3PLS-DYW complexed with RIP2 or RP9 may give us some clues to the reason of RIP9 better efficiency. At a position closest to the L repeat of dsn3PLS, a phenylalanine (157) is present in RIP2 while a tryptophan (160) is present in RIP9 (Supplementary Fig. S8D). This difference might explain the slightly better affinity of RIP9 and dsn3PLS-DYW for *rpoA* in the REMSA. This observation might also explain the co-existence of both RIP2 and RIP9 in plants even though these two proteins are mostly functionally redundant. Most of the *Arabidopsis* plastid editing sites are similarly affected by mutation in either genes encoding for these two RIP proteins [16]. Nevertheless, there are a few sites, including *rpoA*-C200, which exhibit a different effect on their editing extent in the *rip2* or *rip9* mutant plants. For instance, the editing extent of *psbE*-C214 is significantly reduced in the *rip2* mutant while not affected in the *rip9* mutant compared to the wild-type plant [16]. This different outcome might be mediated like for *rpoA*-C200 by a differential affinity of the two RIP proteins for the PPR-PLS protein recognizing *psbE*-C214.

Unexpectedly, we did not detect any gel shift when we assayed ORRM1 with target RNA (Fig. 4B). In a previous study, ORRM1 fused to the maltose binding protein (MBP) was shown to bind near several editing sites by REMSAs [17]. However, we did not see any protein binding when our His-tagged ORRM1 was mixed with the RNA target or both the RNA target and the PPR editing factor (Fig. 4). It is possible that purification of ORRM1 by nickel affinity has negatively affected ORRM1 activity. We tried to use ORRM1 fused to the MBP tag at its *N*-terminus. Even though this tag is much bigger than the His tag (42 versus 0.8 Kd), the MBP-ORRM1 was able to result in 25% editing of the *rpoA*-C200 target when co-expressed with the synthetic factor (Supplementary Fig. S10). Unfortunately, we were not able to detect a shift of the *rpoA* RNA probe with the MBP-ORRM1 protein after many attempts of purifying the protein under different conditions. Given our previous results of ORRM1 binding not only to RNA targets but also to PPR-PLS editing factors [17], we believe that the most likely explanation for the apparent lack of shift of the RNA *rpoA* probe by ORRM1 with or without dsn3PLS-DYW is caused by abnormalities in the protein's properties arising from its purification. The mode of action of ORRM1 in allowing the editing of the *rpoA*-C200 in bacteria in the presence of the synthetic factor might also be different from the RIP proteins. While the RIP proteins bind to the synthetic factor, changing its conformation, resulting in an improved affinity for the RNA, the dual ability of ORRM1 to bind RNA targets and PPR-PLS factors might result in this protein acting like a bridge between the RNA target and the synthetic factor. Nevertheless, we showed that the presence of ORRM1 improves RIP2's ability to enhance the RNA binding activity of the synthetic factor (Fig. 5). This result reinforces the relationship between the editing efficiency observed in bacteria and the RNA binding affinity of dsn3PLS-DYW. The higher the RNA binding affinity of the PPR factor for its target, the higher the editing extent in the bacterial expression system. Given the redundancy of the function of RIP2 and RIP9 on editing of the *rpoA*-C200 target, supported by the lack of additive effect when co-expressed (Fig. 3D), their high similarity and a similar additive effect in the presence of ORRM1 (Fig. 3A–C), it is very likely that ORRM1 affects RIP2 and RIP9 similarly, by improving the ability of the ac-

cessory protein in enhancing the RNA binding activity of the synthetic factor.

The pET-Duet expression system we used to co-express the synthetic factor and various combinations of accessory proteins in *E. coli* turned out to be a judicious choice in order to identify possible off-target events. This system, which is based on compatible vectors with different origin of replication and resistance makers, allowed the simultaneous and comparable expression of the synthetic editing factor and accessory proteins. As a result, we were able to identify a total of 34 different off-target editing events across all the bacterial samples analyzed.

The same synthetic factor and one of the accessory proteins assayed in this work, RIP2, had been assayed previously in bacteria [14]. However, in this previous report, no off-target events were detected. The authors proposed two explanations. First, the target transcript under the control of a strong T7 promoter is very abundant and may sequester a large fraction of the editing factor. This possibility also exists in our system. Second, the co-expression of RIP2 in their experiments reduced PPR protein expression by more than an order of magnitude. This drastic reduction of the expression of the synthetic factor when co-expressed with RIP2 was caused by the use of two vectors, pETM20 and pETM11, respectively, that possess the same origin of replication. As a result, these two vectors competed for the expression machinery. Another factor possibly contributing to our increased detection of off-targets is that our depth coverage is three times higher than in the previous report (an average of 90 million mapped reads/sample, Supplementary Table S4).

The number of off-targets events identified in our study is comparable to what has been observed by expressing two moss editing factors in bacteria, PPR56 and PPR65 [9]. RNA-seq transcriptome analyses after expression of the two editing factors revealed only seven off-targets for PPR65, most with editing efficiencies below 10%, but 79 sites of C-to-U editing for editing factor PPR56. However, the RIP-independent moss editing factors have reduced specificity because their L-motifs are unable to distinguish between different bases as the off-target sites generally show any of A, C, G, or U aligned with the L-motifs in their proteins [9, 30]. The picture is quite different with dsn3PLS-DYW in the presence of accessory proteins, because the L motif at position-14 predominantly binds to the expected U based on the recognition code (Fig. 6). This observation likely results from the interaction of the synthetic factor with either RIP2 or RIP9. Unlike in the P and S motifs, the 35th residue of the L motif is shifted away from the 5th residue, a misalignment that is corrected by RIP9 [25]. The analysis of the off-target upstream sequences revealed other positions, such as -13, -9, -7, and -6, which are in very good agreement with the PPR recognition code (Fig. 6). The PPR code has been established by aligning PPR proteins with their target sequences and comparing the co-occurrence of aa in their fifth and last position with their associated nucleotides [11, 31, 32]. The positions at -5 (T/R) and -4 (G/N) are neutral or slightly favored; nevertheless, there is a very strong bias toward A at these positions. In sample 6, which co-expresses the synthetic factor with ORRM1 and RIP2, 18 of the 19 of the off-target upstream sequences contain an A at position -4 (Fig. 6A). The same bias was observed in the off-targets identified in the chloroplast transcriptome after dsn3PLS-DYW was introduced in a *clb19* mutant background [14]. Clearly, the PPR code needs to be refined to be able to explain this re-

sult. Although there has been strong experimental support for the involvement of the E domain in PPR–PLS–RNA interaction [33], we did not observe any strong bias at positions  $-3$  and  $-2$  aligning with the E1 and E2 motifs of dsn-3PLS-DYW (Bottom logo Fig. 6B).

Another limitation of the PPR code is the assumption of an absence of context in the favorability of the binding to a certain ribonucleotide. Clearly, this assumption is proved wrong in considering the L motif (P/D), which at position  $-14$  binds preferentially U as predicted but at position  $-8$  binds predominantly G (Fig. 6A and B). Other positions deviating from the expected nucleotide based on the PPR code are  $-15$  and  $-10$ . This type of data should be helpful for optimizing future designs by replacing the specificity determining aa at these positions by other combinations. Since the PPR code is degenerate, N/D or P/D are equally favorable to bind U [32]. P/D could be tried at position  $-15$  while N/D could be tried at position  $-8$ . However, modifying the specificity of a PPR motif can also have impact on the specificity of other PPR motifs, especially at upstream positions, again emphasizing that the assumption of independence in the specificity of each PPR motif is oversimplistic [30]. We applied the PPR code to predict binding sites for the PLS motifs of the synthetic factor within the coding sequences of *E. coli* using the Preact Tool TargetScan [34] (Supplementary Fig. S11). Only two of the predicted dsn3PLS-DYW cytidines targets were observed in our RNA-seq analysis. We verified that the level of expression of these predicted targets was sufficient for editing to be detected in our RNA-seq analysis (Supplementary Fig. S12). The poor predictive value of the PPR code clearly underscores that many factors can blur its predictability by limiting the accessibility of targets by the editosome such as RNA secondary structure or protection by other RNA-binding proteins.

This work legitimizes the use of a synthetic factor in a heterologous system in order to study the contribution of accessory proteins in the function of the angiosperm editosome. We have demonstrated the independent involvement of RIP2 (or RIP9) with ORRM1 in the activity of this molecular apparatus. We were able to show that the higher efficiency of RIP9 versus RIP2 in editing could be reliably linked to a higher affinity of the synthetic factor for its RNA target. We have also shown that an improved efficiency brought by the accessory proteins is accompanied by a concurrent lack of selectivity because the number of off-targets increases. Despite these new findings, there are inherent limitations to the system we used that come from either the heterologous system or the synthetic factor. The lack of activity of two of the 5 accessory proteins assayed, OZ1 and ISE2 might come from a lack of PTMs present in plant organelles but absent in bacteria. Alternatively, the synthetic factor may be different enough from the natural PPR factor that it does not require the functions of OZ1 and ISE2 anymore to fulfill the editing of the *rpoA*-C200 target. One way to investigate this possibility would be to study the knockout (knockdown) effect of OZ1 (ISE2) in a dsn3PLS-DYW complemented *clb19* mutant line, an approach far beyond the scope of this work. It remains to be seen whether testing this system in human cells, as has been done for the moss factor, will result in hundreds of off-targets as observed with the moss PPR proteins, or whether plant accessory proteins will affect the level of off-target editing.

## Acknowledgements

The authors are very grateful for technical assistance by the RNA core facility at Cornell University.

*Author contributions:* J.L., M.R.H., and S.B. designed and conceived the experiments. J.L. and S.B. performed the *E. coli* experiments. J.L. performed bioinformatic analysis. J.L., M.R.H., and S.B. analyzed the results. S.B. supervised the work and drafted the manuscript. M.R.H. and S.B. edited the manuscript.

## Supplementary data

Supplementary data are available at NAR online.

## Conflict of interest

None declared.

## Funding

This work was supported by the National Science Foundation Division of Molecular and Cellular Biosciences [MCB-2122032 to S.B.]. Funding to pay the Open Access publication charges for this article was provided by National Science Foundation Division of Molecular and Cellular Biosciences Genetic Mechanisms [MCB-2122032 to S.B.].

## Data availability

The RNAseq data have been deposited in the SRA archive as BioProject PRJNA1152098. The custom scripts have been deposited and are accessible with DOI:10.5281/zenodo.13381645.

## References

1. Small ID, Schallenberg-Rudinger M, Takenaka M *et al.* Plant organellar RNA editing: what 30 years of research has revealed. *Plant J* 2020;101:1040–56. <https://doi.org/10.1111/tpj.14578>
2. Bentolila S, Oh J, Hanson MR *et al.* Comprehensive high-resolution analysis of the role of an *Arabidopsis* gene family in RNA editing. *PLoS Genet* 2013;9:e1003584. <https://doi.org/10.1371/journal.pgen.1003584>
3. Barkan A, Small I. Pentatricopeptide repeat proteins in plants. *Annu Rev Plant Biol* 2014;65:415–42. <https://doi.org/10.1146/annurev-arplant-050213-040159>
4. Okuda K, Nakamura T, Sugita M *et al.* A pentatricopeptide repeat protein is a site recognition factor in chloroplast RNA editing. *J Biol Chem* 2006;281:37661–7. <https://doi.org/10.1074/jbc.M608184200>
5. Wagoner JA, Sun T, Lin L *et al.* Cytidine deaminase motifs within the DYW domain of two pentatricopeptide repeat-containing proteins are required for site-specific chloroplast RNA editing. *J Biol Chem* 2015;290:2957–68. <https://doi.org/10.1074/jbc.M114.622084>
6. Hayes ML, Dang KN, Diaz MF *et al.* A conserved glutamate residue in the C-terminal deaminase domain of pentatricopeptide repeat proteins is required for RNA editing activity. *J Biol Chem* 2015;290:10136–42. <https://doi.org/10.1074/jbc.M114.631630>
7. Boussardon C, Salone V, Avon A *et al.* Two interacting proteins are necessary for the editing of the NdhD-1 site in *Arabidopsis* plastids. *Plant Cell* 2012;24:3684–94. <https://doi.org/10.1105/tpc.112.099507>

8. Sun T, Bentolila S, Hanson MR. The unexpected diversity of plant organelle RNA editosomes. *Trends Plant Sci* 2016;21:962–73. <https://doi.org/10.1016/j.tplants.2016.07.005>
9. Oldenkott B, Yang Y, Lesch E *et al.* Plant-type pentatricopeptide repeat proteins with a DYW domain drive C-to-U RNA editing in *Escherichia coli*. *Commun Biol* 2019;2:85. <https://doi.org/10.1038/s42003-019-0328-3>
10. Barkan A, Rojas M, Fujii S *et al.* A combinatorial amino acid code for RNA recognition by pentatricopeptide repeat proteins. *PLoS Genet* 2012;8:e1002910. <https://doi.org/10.1371/journal.pgen.1002910>
11. Yagi Y, Hayashi S, Kobayashi K *et al.* Elucidation of the RNA recognition code for pentatricopeptide repeat proteins involved in organelle RNA editing in plants. *PLoS One* 2013;8:e57286. <https://doi.org/10.1371/journal.pone.0057286>
12. Coquille S, Filipovska A, Chia T *et al.* An artificial PPR scaffold for programmable RNA recognition. *Nat Commun* 2014;5:5729. <https://doi.org/10.1038/ncomms6729>
13. Gully BS, Shah KR, Lee M *et al.* The design and structural characterization of a synthetic pentatricopeptide repeat protein. *Acta Crystallogr D Biol Crystallogr* 2015;71:196–208. <https://doi.org/10.1107/S1399004714024869>
14. Royan S, Gutmann B, Colas des Franks-Small C *et al.* A synthetic RNA editing factor edits its target site in chloroplasts and bacteria. *Commun Biol* 2021;4:545. <https://doi.org/10.1038/s42003-021-02062-9>
15. Chateigner-Boutin AL, Ramos-Vega M, Guevara-Garcia A *et al.* CLB19, a pentatricopeptide repeat protein required for editing of *rpoA* and *clpP* chloroplast transcripts. *Plant J* 2008;56:590–602. <https://doi.org/10.1111/j.1365-313X.2008.03634.x>
16. Takenaka M, Zehrmann A, Verbitskiy D *et al.* Multiple organellar RNA editing factor (MORF) family proteins are required for RNA editing in mitochondria and plastids of plants. *Proc Natl Acad Sci USA* 2012;109:5104–9. <https://doi.org/10.1073/pnas.1202452109>
17. Sun T, Germain A, Giloteaux L *et al.* An RNA recognition motif-containing protein is required for plastid RNA editing in *Arabidopsis* and maize. *Proc Natl Acad Sci USA* 2013;110:E1169–1178. <https://doi.org/10.1073/pnas.1220162110>
18. Sun T, Shi X, Friso G *et al.* A zinc finger motif-containing protein is essential for chloroplast RNA editing. *PLoS Genet* 2015;11:e1005028. <https://doi.org/10.1371/journal.pgen.1005028>
19. Bobik K, McCray TN, Ernest B *et al.* The chloroplast RNA helicase ISE2 is required for multiple chloroplast RNA processing steps in *Arabidopsis thaliana*. *Plant J* 2017;91:114–31. <https://doi.org/10.1111/tpj.13550>
20. Guillaumot D, Lopez-Obando M, Baudry K *et al.* Two interacting PPR proteins are major *Arabidopsis* editing factors in plastid and mitochondria. *Proc Natl Acad Sci USA* 2017;114:8877–82. <https://doi.org/10.1073/pnas.1705780114>
21. Xu L, Liu Y, Han R. BEAT: a Python program to quantify base editing from sanger sequencing. *CRISPR J* 2019;2:223–9. <https://doi.org/10.1089/crispr.2019.0017>
22. Mirdita M, Schutze K, Moriwaki Y *et al.* ColabFold: making protein folding accessible to all. *Nat Methods* 2022;19:679–82. <https://doi.org/10.1038/s41592-022-01488-1>
23. Pettersen EF, Goddard TD, Huang CC *et al.* UCSF Chimera—a visualization system for exploratory research and analysis. *J Comput Chem* 2004;25:1605–12. <https://doi.org/10.1002/jcc.20084>
24. Piechotta M, Naarmann-de Vries IS, Wang Q *et al.* RNA modification mapping with JACUSA2. *Genome Biol* 2022;23:115. <https://doi.org/10.1186/s13059-022-02676-0>
25. Yan J, Zhang Q, Guan Z *et al.* MORF9 increases the RNA-binding activity of PLS-type pentatricopeptide repeat protein in plastid RNA editing. *Nat Plants* 2017;3:17037. <https://doi.org/10.1038/nplants.2017.37>
26. Bentolila S, Heller WP, Sun T *et al.* RIP1, a member of an *Arabidopsis* protein family, interacts with the protein RARE1 and broadly affects RNA editing. *Proc Natl Acad Sci USA* 2012;109:E1453–1461. <https://doi.org/10.1073/pnas.1121465109>
27. Hackett JB, Shi X, Kobylarz AT *et al.* An organelle RNA recognition motif protein is required for photosystem II subunit *psbF* transcript editing. *Plant Physiol* 2017;173:2278–93.
28. Shi X, Castanet B, Germain A *et al.* ORRM5, an RNA recognition motif-containing protein, has a unique effect on mitochondrial RNA editing. *J Exp Bot* 2017;68:2833–47. <https://doi.org/10.1093/jxb/erx139>
29. Shi X, Hanson MR, Bentolila S. Two RNA recognition motif-containing proteins are plant mitochondrial editing factors. *Nucleic Acids Res* 2015;43:3814–25. <https://doi.org/10.1093/nar/gkv245>
30. Lesch E, Schilling MT, Brenner S *et al.* Plant mitochondrial RNA editing factors can perform targeted C-to-U editing of nuclear transcripts in human cells. *Nucleic Acids Res* 2022;50:9966–83. <https://doi.org/10.1093/nar/gkac752>
31. Takenaka M, Zehrmann A, Brennicke A *et al.* Improved computational target site prediction for pentatricopeptide repeat RNA editing factors. *PLoS One* 2013;8:e65343. <https://doi.org/10.1371/journal.pone.0065343>
32. Kobayashi T, Yagi Y, Nakamura T. Comprehensive prediction of target RNA editing sites for PLS-class PPR proteins in *Arabidopsis thaliana*. *Plant Cell Physiol* 2019;60:862–74. <https://doi.org/10.1093/pcp/pcy251>
33. Ruwe H, Gutmann B, Schmitz-Linneweber C *et al.* The E domain of CRR2 participates in sequence-specific recognition of RNA in plastids. *New Phytol* 2019;222:218–29. <https://doi.org/10.1111/nph.15578>
34. Lenz H, Hein A, Knoop V. Plant organelle RNA editing and its specificity factors: enhancements of analyses and new database features in PREPACT 3.0. *BMC Bioinf* 2018;19:255. <https://doi.org/10.1186/s12859-018-2244-9>